Comparison of liquid hydrogen tank performance at different storage pressures and operational scenarios using a reduced-order model

K R Appel, K I Matveev, and J W Leachman

HYdrogen Properties for Energy Research (HYPER) Center, School of Mechanical and Materials Engineering, Washington State University, Pullman, WA 99164-2920 USA

Corresponding Author. Email: jacob.leachman@wsu.edu

Abstract. Liquid hydrogen storage is accompanied by boil-off losses as heat penetrates the tank. However, these losses are also affected by tank operational scenarios which have been relatively unconsidered in the literature. To address this need, a reduced-order model capable of analyzing different operational scenarios was developed. Using this model, the present study investigates the effects of storage pressure in vertical and horizontal storage tanks on the average daily boil-off losses. Parametric studies are conducted using the dimensions of the Integrated Refrigeration and Storage (IRAS) system tank with varied venting pressure, fill level, and initial temperature of the liquid in the tank. The results indicate that storing saturated liquid hydrogen at lower pressures with no liquid extraction from the tank in steady-state cyclic venting results in lower daily losses. The initial temperature of the liquid in the tank also plays a key role in selecting a storage pressure for a tank. With no liquid subcooling, lower storage pressures are desirable but with 1 K subcooled liquid higher storage pressures with larger fill levels result in lower losses. The resulting model is a useful tool for analyzing different liquid hydrogen tank operational scenarios.

1. Introduction

Hydrogen is a clean and renewable fuel that naturally exists as a gas, but if cooled to cryogenic temperatures (20 K, -420°F) it changes phases from a gas to a liquid. Through liquefaction, a higher storage density is attained compared to compressed gas. However, due to the low storage temperature, a high thermal gradient exists between the inside of the tank and the ambient environment leading to heat transfer through the tank walls. As heat penetrates the tank, the liquid is evaporated resulting in self-pressurization of the tank, as the vapor expands to fill more space than liquid. Pressure in the tank continues to rise forcing pressure relief devices (PRDs) to vent vapor from the tank to reduce the pressure and maintain safety. As a result of the self-pressurization, the venting of vapor is a cyclic process that accounts for 0.1%-3.0% of the total mass of hydrogen lost per day, showing the important need for a reduction in hydrogen losses [1,2]. Typical tanks store up to 4300 kg of LH2, and if 3% of the total mass is lost per day, then on the first day of storage, up to 129 kg of hydrogen will be vented. Assuming hydrogen costs around $11/kg in the tank, then $1,419 is lost on the first day alone [3].

Plug Power has estimated that 7%-25% of an LH2 load is lost [4]. Using the same 4300 kg tank load that means of the 4300 kg stored, up to 1067 kg is lost per load, amounting to $11,737 per load lost. The International Energy Agency estimates that the hydrogen demand compared to 2020 will increase almost six times to 530 Mt in 2050 [5]. Given the projected future demand, the need is clear to make LH2 storage more economical.

Numerical models are often used to predict the self-pressurization of liquid hydrogen storage tanks, exploring the effect of tank size, and some effects of tank operations [6,7]. A numerical model utilized in this work is aimed to investigate the effect of storage pressure on boil-off losses. Using the model, the influence of initial superheating of the vapor and subcooling of the liquid are explored with varied storage pressures in vertical and horizontal tanks. Comparisons are then made between the storage pressures for conditions where losses are minimized.

2. Model

Conservation of mass and energy equations are applied to the bulk fluid nodes using heat and mass transfer terms crossing the boundary to evaluate tank pressure.

$$\frac{dm}{dt} = \sum_j \dot{m}_j \tag{1}$$

where, $\frac{dm}{dt}$ is the change in mass of the node over time and $\dot{m}_j$ is any mass flow crossing node boundaries. In this model, the specific enthalpy form of the energy equation is employed:

$$m\frac{d\bar{h}}{dt} = \sum_i \dot{Q}_i + \sum_j \dot{m}_j\left(h_j - \bar{h}\right) + V\frac{dP}{dt} \tag{2}$$

where, $\frac{d\bar{h}}{dt}$ is the change in average enthalpy of the node over time, $\dot{Q}_i$ is any heat flow crossing node boundaries, $\left(h_j - \bar{h}\right)$ is the difference between the enthalpy of a mass flow crossing node boundaries and the average enthalpy of the node, V is the volume of the node, and $\frac{dP}{dt}$ is the change in pressure in the node over time. The heat and mass transfer terms are summarized in Table 1. To find the heat transfer at the interface for the vapor and liquid nodes Newton's law of cooling is utilized:

$$\dot{Q}_{V,LI} = \hat{h}_{V,LI}A_I\left(T_{V,L} - T_I\right) \tag{3}$$

where, $\dot{Q}_{V,LI}$ is the heat transfer due to convection at the interface, A_I is the area of the interface between liquid and vapor nodes, and $\left(T_{V,L} - T_I\right)$ is the difference between the temperature of the node and the interface temperature. The natural convection coefficient can be found with the standard correlation [6,8]:

$$\hat{h}_{V,LI} = kC\frac{\lambda}{L}Ra^n \tag{4}$$

where, k is a model calibration coefficient, C and n are 0.27 and 0.25 respectively, λ is the thermal conductivity, L is the characteristic vertical height of the node, and Ra is found as a product of the Prandtl and Grashof numbers. In the model, the Prandtl number, as well other hydrogen properties, is found using a NIST database REFPROP[9–11]. The Grashof number is given by the equation [6]:

$$Gr = \frac{L^3\rho^2 g\beta\Delta T}{\mu^2} \tag{5}$$

where ΔT is the characteristic temperature difference between the interface and the node, g is the acceleration due to gravity, ρ is the density, β is the volumetric expansivity, and μ is the viscosity. The energy and mass conservation equations are numerically integrated in MATLAB with heat and mass transfer terms to determine the mass and specific enthalpy in the node after a timestep. All needed properties are obtained via REFPROP [9–11]. The calibration coefficient above is optimized with experimental data from the IRAS tank to minimize the average deviation between the model prediction and experimental data [7].

Tank dimensions for the model validation are based on the Integrated Refrigeration and Storage (IRAS) system [12], which utilizes a horizontal cylindrical tank with an internal length 21.8 m, a diameter of 2.9 m, and 2:1 elliptical heads for a total liquid hydrogen volume of 125 m^3. The reduced-order model utilizes three

nodes for the bulk liquid and vapor, and the infinitely thin interface between the two with saturated properties. The mass and heat transfer mechanisms into the nodes is shown in Figure 1.

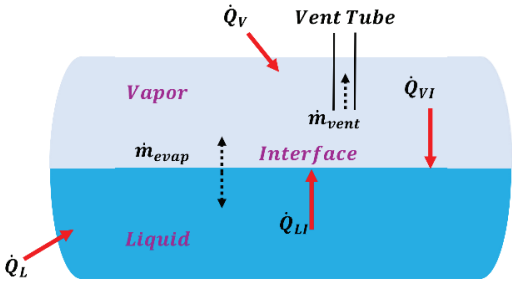

Figure 1. Model diagram for a horizontal cylindrical tank with heat and mass transfer terms.

Table 1. Summarized heat and mass transfer terms used in the model.

Symbol	Definition
$\dot{Q}_V$	Heat transfer through the tank to the vapor node
$\dot{Q}_L$	Heat transfer through the tank to the liquid node
$\dot{Q}_{LI}$	Heat transfer at the interface from the liquid node
$\dot{Q}_{VI}$	Heat transfer at the interface from the vapor node
$\dot{Q}_{Lext}$	Heat extraction from the liquid node
$\dot{Q}_{Vext}$	Heat extraction from the vapor node
$\dot{m}_{vent}$	Venting mass transfer from vapor node[1]
$\dot{m}_{evap}$	Mass transfer from evaporation from liquid to vapor node (positive indicates evaporation, negative indicates condensation)
	[1]Controlled parameter via calibration

3. Results

3.1 Model validation

The model is validated using experimental data from IRAS and the Multi-purpose Hydrogen Test Bed (MHTB) [12,13]. During the validation an average optimal calibration coefficient is found to predict the datasets from the two experimental tanks with the least amount of error. The mean average percent error with the average calibration coefficient for the MHTB, a vertical cylindrical tank, and the IRAS, a horizontal cylindrical tank, are ±4.3% and ±3.6% respectively. A more thorough validation explanation can be found in the thesis from source [7].

3.2 Parametric study setup

After validation, parametric studies are carried out to investigate the effect of initial conditions and storage pressure on the average daily boil-off losses. The tank is analyzed in both horizontal and vertical configurations with initial conditions summarized in Table 2. To maintain consistency, the initial pressure is 96% of the venting pressure. The closing pressures for each case are 77.5 kPa lower than the opening pressure.

Table 2. Parametric study initial conditions for vapor and liquid temperatures and venting pressure.

Venting Pressure (kPa) (absolute)	Initial vapor superheating (K)	Initial liquid subcooling (K)
239, 515, 791, 1067	1	0
239, 515, 791, 1067	1	1
239, 515, 791, 1067	4	0
239, 515, 791, 1067	4	1

To find the average daily losses incurred from venting, the model predicts cyclic venting until flash evaporation occurs, a condition where the liquid temperature reaches the saturation temperature. When this condition is met, steady-state cyclic venting occurs, and the time duration and losses for one venting cycle are extrapolated as the average daily losses. Time-dependent pressure traces are shown in Figure 2 for the highest-pressure case using the highest and lowest fill levels with and without subcooling of the liquid to see the effects on the pressure in the tank.

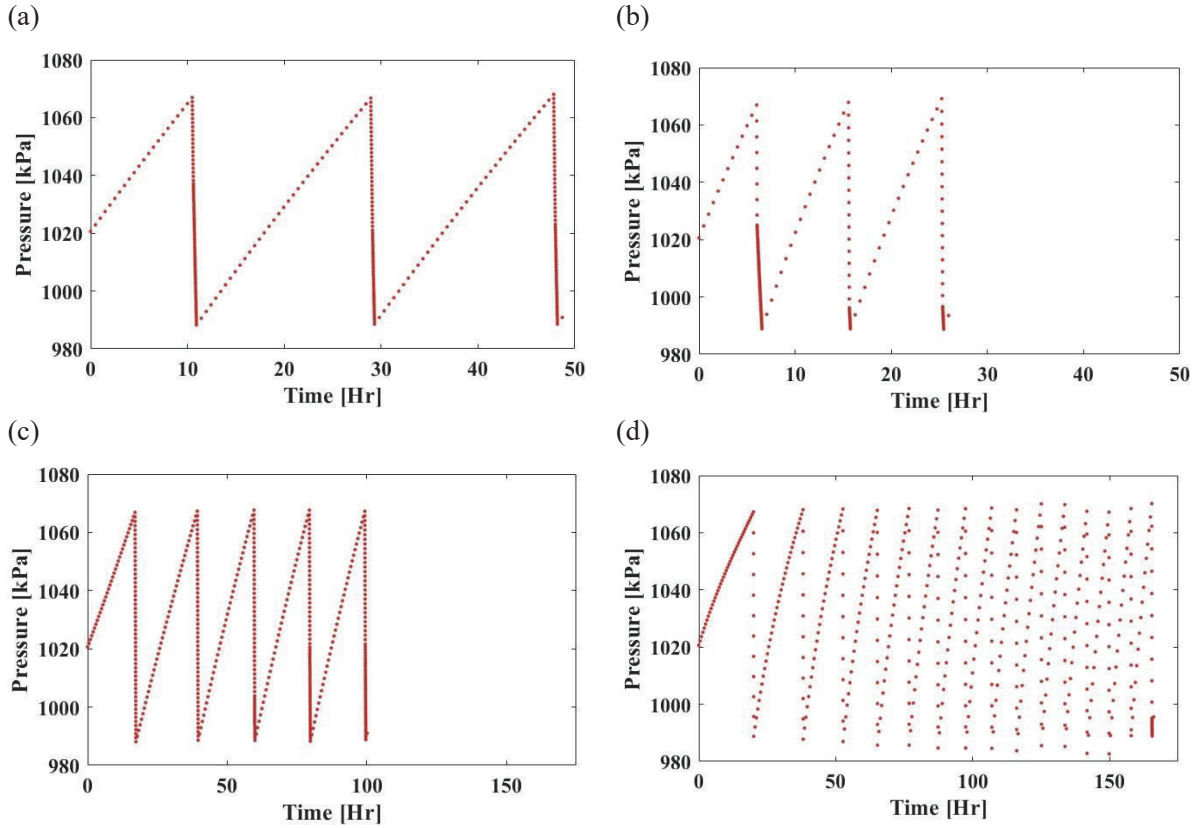

Figure 2. Time-dependent pressure traces with 1067 kPa venting and initial conditions: (a) 1 K superheated vapor and low fill level, (b) 1 K superheated vapor and high fill level, (c) 1 K superheated vapor, 1 K subcooled liquid, and low fill level, (d) 1 K superheated vapor, 1 K subcooled liquid, and high fill level.

Comparing the low and high fill levels with 1 K superheated vapor (Figure 2a and Figure 2b), the time to reach steady state venting is much shorter with the high fill level. With less volume for vapor above the liquid, evaporation leads to a faster pressurization rate. This trend is reversed when the liquid is initially subcooled shown in Figure 2c and Figure 2d. In Figure 2c five cyclic vent cycles are shown over 100 hours to reach steady state venting whereas 15 cycles are shown in Figure 2d in 165 hours of simulation. Due to

the large volume of subcooled liquid, it takes longer for the tank to reach steady-state cyclic venting. Flash evaporation is shown in the pressure traces by the denser populations of data points near the end of a vent, which is caused by an increased evaporation rate resulting in reduced pressure drop during venting. In the plots with subcooled liquid, flash evaporation occurs after several cyclic vents, indicating a lower transient boil-off loss compared to the saturated cases. The longer the period before steady state cyclic venting the lower the overall losses will be for the tanks.

3.3 Horizontal tank results

The calculated average daily losses for the horizontal tank with varied conditions are shown in Figure 3 with fill level percent by volume. As expected, increasing the fill level at the start of the simulation results in higher losses due to the reduced volume available for vapor. The results also show that under steady-state conditions lower storage pressures tend to have lower average losses but are more sensitive to increased fill level compared to the other pressures. This is contrary to a previous work which analyzed tanks with liquid extraction operations and considered the transient losses of the tank [7]. During the first venting cycle, the amount of hydrogen vented highly depends on the initial temperature of the liquid. If the temperature starts at saturation, then a large amount of hydrogen is vented during the first cyclic vent because the temperature of the liquid quickly reaches the saturation temperature, causing a flash evaporation event which results in a high evaporation rate. For this reason, this work specifically explores the effects of the initial conditions once the tank reaches steady-state operation.

Superheating the vapor by 4 K compared to 1 K tends not to affect the boil-off losses for the 239 kPa storage pressure but affects higher storage pressures at lower fill levels. Venting pressures greater than 239 kPa resulted in decreased losses at low fill levels but increased almost linearly to similar maximum losses. One cause for the decrease in losses is attributed to the density of the vented hydrogen. When hydrogen vapor is vented close to or at saturation, more mass must be released for a set volume compared to a lower density flow. So having higher temperature vapor vented reduces the total amount of mass that must be released to decrease the pressure. Another cause for the decreased losses with 4 K superheating is the enthalpy of the vented hydrogen. As higher enthalpy hydrogen leaves the tank a greater amount of energy is leaving the vapor node in a temperature reduction. Increasing the superheating to 4 K also reduces the gap in losses between the storage pressures for lower fill levels. Less liquid in the tank results in a larger volume of high temperature vapor resulting in lower density hydrogen being vented. Greater volumes of liquid results in quicker temperature reduction of the vapor and venting of higher density hydrogen. Subcooling the liquid by 1 K results in a small increase in average daily losses for the 239 kPa storage pressure. In the 515 kPa storage pressure, subcooling the liquid decreases the losses with fill levels below 80%. Across all fill levels, the losses decrease for the 1 K subcooled liquid with 791 and 1067 kPa storage pressures compared to the initial superheated case.

While the steady-state losses are the focus of this study, the time for steady-state to be reached was also calculated. Steady-state cyclic venting is achieved when the temperature of the liquid reaches saturation during a vent; before this condition all cyclic venting has lower daily loss rates. Longer times to steady-state result in less overall losses from the tank due to the lack of rapid evaporation events. Comparing studies with superheated vapor and subcooled liquid shows that subcooling the liquid greatly increases the time required to reach steady-state venting. The 239 kPa storage pressure consistently has lower times to reach steady-state conditions, indicating fewer transient cycles with lower losses, and more flash evaporation. The study with 1067 kPa has the longest time to reach steady-state, taking 161 hours with 4 K superheated vapor and 1 K subcooled liquid.

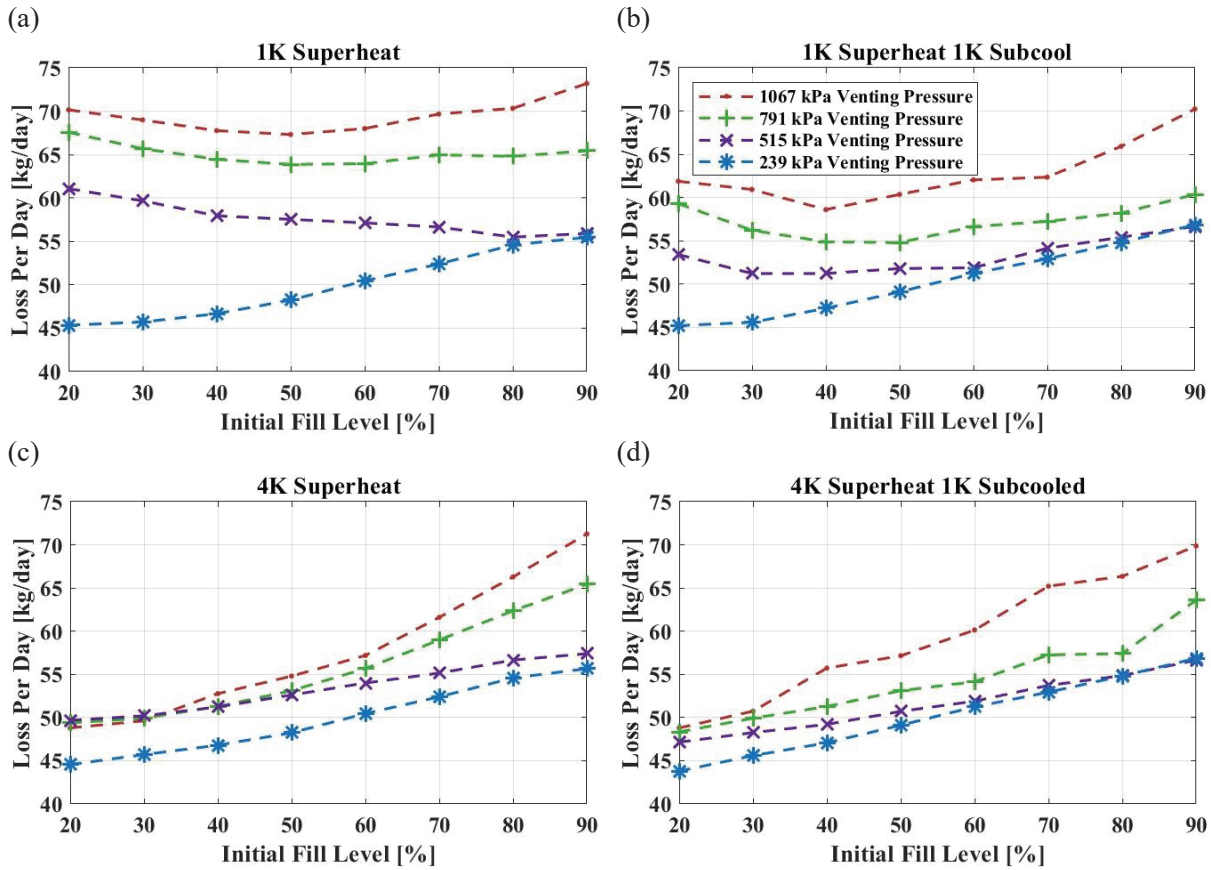

Figure 3. Parametric results for a horizontal cylindrical tank with varied pressure and initial conditions: (a) 1 K superheated vapor, (b) 1 K superheated vapor, and 1 K subcooled liquid, (c) 4 K superheated vapor, (d) 4 K superheated vapor, and 1 K subcooled liquid.

3.4 Vertical tank results

The trends in losses for vertical tanks are different than horizontal tanks as shown in Figure 4. Lower losses tend to be maintained until higher fill levels compared to the horizontal tank, but when the losses start to increase the rate of change is greater than in the horizontal tank at higher fill levels. In the vertical tank the higher storage pressure results in higher losses. The three storage pressures above 239 kPa decrease with increasing fill level until the tank is 70-80% full after which the losses are predicted to increase. Because this work only considers the steady state venting instead of including transient losses, the results are contrary to the work previously analyzing the effect of tank pressures [7]. Increasing the superheating from 1 K to 4 K shows a smaller decrease in losses with venting pressures of 515, 791, and 1067 kPa compared to the horizontal tank, but the reduced losses propagate into higher fill levels. The 239 kPa storage pressure is again less sensitive to the superheating of the vapor decreasing only slightly.

Subcooling the liquid by 1 K in the vertical tank has more effect on the losses in the vertical tank than in the horizontal tank. The smaller interface area proves to decrease the amount of heat exchange between liquid and vapor resulting in lower losses until higher fill levels. At higher fill levels the large amount of liquid results in cooling of the vapor to near saturation. As a result, when venting takes place high density and relatively high enthalpy vapor is vented, removing more mass and energy for the same volume compared to the 1 K superheated vapor case. The times to reach steady-state for the vertical tank are far more consistent

with less pronounced trends than in the horizontal tank configuration. The longer period before steady-state cyclic venting shows decreased losses due to the lack of flash evaporation which increases the self-pressurization rate of the tank. The maximum time to reach steady-state was 173 hours with initial tank conditions of 4 K superheated vapor, 1 K subcooled liquid, and storage pressure of 1067 kPa.

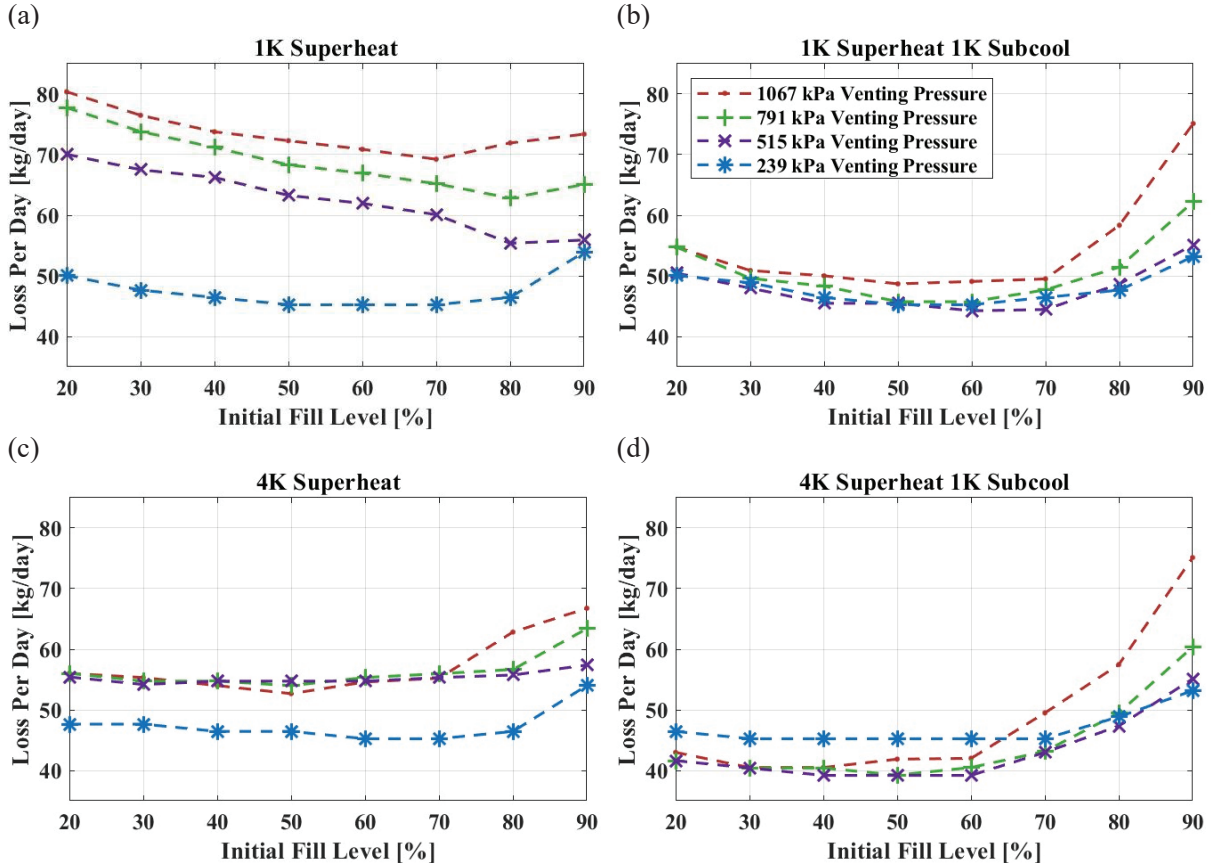

Figure 4. Parametric results for a vertical cylindrical tank with varied pressure and initial conditions: (a) 1K superheated vapor, (b) 1 K superheated vapor, and 1 K subcooled liquid, (c) 4 K superheated vapor, (d) 4 K superheated vapor, and 1 K subcooled liquid.

The average daily losses are calculated for each of the studies for both configurations showing general trends for the tanks. Tanks with no subcooling and 1 K superheated vapor the average daily losses for vertical tanks are higher for all pressures except 239 kPa. When the liquid is subcooled by 1 K the vertical tank always has the lowest daily average losses. Superheating the vapor by 4 K makes the average losses for both vertical and horizontal tanks close in value except for the 239 kPa scenario, where the vertical tank has lower average daily losses. The model predicts that average daily losses for the vertical tank are lower at all pressures when the vapor is superheated by 4 K and the liquid is subcooled by 1 K. The average daily losses are shown in Table 3 for the various combinations of tank orientation and initial conditions.

Table 3. Average daily losses for horizontal and vertical tanks with varied initial hydrogen conditions.

Configuration	Storage Pressure	Average daily losses (kg/day)			
		1 K superheated vapor	1 K superheated vapor, 1 K subcooled liquid	4 K superheated vapor	4 K superheated vapor, 1 K subcooled liquid
Horizontal	1067 kPa	68.0	62.8	57.8	59.2
Vertical	1067 kPa	73.5	54.6	57.2	48.7
Horizontal	791 kPa	61.7	57.2	55.8	54.4
Vertical	791 kPa	68.9	50.7	56.4	44.4
Horizontal	515 kPa	54.8	53.2	53.4	51.6
Vertical	515 kPa	62.6	47.7	55.3	43.1
Horizontal	239 kPa	49.3	50.4	49.8	50.2
Vertical	239 kPa	47.5	47.9	47.4	46.8

4. Conclusions

The effect of internal storage pressure with various initial conditions for the hydrogen in the tank is investigated using a reduced-order model. The model is validated with vertical cylindrical tank data from the MHTB and horizontal cylindrical tank data from IRAS resulting in ±4.3% and ±3.6% errors, respectively. While lower pressures in steady-state cyclic venting show the lowest losses, in tanks with subcooled liquid, the use of higher pressures decreases the overall losses due to the long period before steady-state cyclic venting. Vertical tanks tend to be more sensitive to the conditions of the hydrogen compared to horizontal tanks and maintain lower losses until higher fill levels. Vertical tanks average lower daily losses when the liquid is subcooled. One potential improvement for this model is the addition of a dedicated thermal stratification model for the ullage which would more accurately predict the temperature of the vented hydrogen without the need to assume all vapor is superheated.

5. References

[1] Zhang F, Zhao P, Niu M, Maddy J. 2016. *Int J Hydrogen Energy*. **41**(33):14535–52. DOI:10.1016/j.ijhydene.2016.05.293.
[2] Decker L. 2019. *HYPER closing seminar*.
[3] Koleva M, Rustagi N. 2020. Available from: hdsam.es.anl.gov/index.php?content=hdsam.
[4] Marsh A. 2019. In: Cryogenic Engineering Conference.
[5] IEA. 2022. *World Energy Outlook 2022.*
[6] Matveev KI, Leachman JW. 2023. *Hydrogen*. **4**(3):444–55. DOI:10.3390/hydrogen4030030.
[7] Appel K. 2024. *Master Thesis.* Washington State University, Pullman.
[8] Bandyopadhyay A, Majumdar AK, Leclair AC, Valenzuela JG. 2019. *AIAA Propulsion and Energy*. DOI:10.2514/6.2019-4122.
[9] Lemmon EW, Bell IH, Huber ML, McLinden MO. 2018. *National Institute of Standards and Technology Standard Reference Data Program.*
[10] Leachman JW, Jacobsen RT, Penoncello SG, Lemmon EW. 2009. *J Phys Chem Ref Data*. DOI:10.1063/1.3160306.
[11] Assael MJ, Assael JAM, Huber ML, Perkins RA, Takata Y. 2011. *J Phys Chem Ref Data*. DOI:10.1063/1.3606499
[12] Swanger A. 2018. *Master Thesis.* University of Central Florida, Orlando.
[13] Hastings LJ, Flachbart RH, Martin JJ, Hedayat A, Fazah M, Lak T, et al. 2003. No. NASA/TM-2003-212926.